

ARTICLE

Received 17 Mar 2015 | Accepted 2 Sep 2015 | Published 13 Oct 2015

DOI: 10.1038/ncomms9533

OPEN

Mucosal vaccination with attenuated *Mycobacterium tuberculosis* induces strong central memory responses and protects against tuberculosis

Deepak Kaushal^{1,2,*}, Taylor W. Foreman^{1,3,*}, Uma S. Gautam¹, Xavier Alvarez¹, Toidi Adekambi^{4,5}, Javier Rangel-Moreno⁶, Nadia A. Golden¹, Ann-Marie F. Johnson¹, Bonnie L. Phillips^{1,3}, Muhammad H. Ahsan¹, Kasi E. Russell-Lodrigue¹, Lara A. Doyle¹, Chad J. Roy¹, Peter J. Didier¹, James L. Blanchard¹, Jyothi Rengarajan^{4,5}, Andrew A. Lackner^{1,2,7}, Shabaana A. Khader⁸ & Smriti Mehra^{1,9,10}

Tuberculosis (TB) is a global pandemic, partially due to the failure of vaccination approaches. Novel anti-TB vaccines are therefore urgently required. Here we show that aerosol immunization of macaques with the *Mtb* mutant in SigH (*Mtb* Δ *sigH*) results in significant recruitment of inducible bronchus-associated lymphoid tissue (iBALT) as well as CD4⁺ and CD8⁺ T cells expressing activation and proliferation markers to the lungs. Further, the findings indicate that pulmonary vaccination with *Mtb* Δ *sigH* elicited strong central memory CD4⁺ and CD8⁺ T-cell responses in the lung. Vaccination with *Mtb* Δ *sigH* results in significant protection against a lethal TB challenge, as evidenced by an approximately three log reduction in bacterial burdens, significantly diminished clinical manifestations and granulomatous pathology and characterized by the presence of profound iBALT. This highly protective response is virtually absent in unvaccinated and BCG-vaccinated animals after challenge. These results suggest that future TB vaccine candidates can be developed on the basis of *Mtb* Δ *sigH*.

¹Tulane National Primate Research Center, Covington, Louisiana 70433, USA. ²Department of Microbiology and Immunology, Tulane Health Sciences Center, New Orleans, Louisiana 70112, USA. ³Biomedical Sciences Graduate Program, Tulane Health Sciences Center, New Orleans, Louisiana 70112, USA. ⁴Yerkes National Primate Research Center, Atlanta, Georgia 30329, USA. ⁵Emory Vaccine Center, Atlanta, Georgia 30329, USA. ⁶University of Rochester Medical Center, Rochester, New York 14642, USA. ⁷Department of Pathology, Tulane Health Sciences Center, New Orleans, Louisiana 70112, USA. ⁸Department of Molecular Microbiology, Washington University at St Louis, St Louis, Missouri 63110, USA. ⁹Center for Biomedical Research Excellence, Louisiana State University School of Veterinary Medicine, Baton Rouge, Louisiana 70803, USA. ¹⁰Department of Pathobiological Sciences, Louisiana State University School of Veterinary Medicine, Baton Rouge, Louisiana 70803, USA. *These authors contributed equally to this work. Correspondence and requests for materials should be addressed to D.K. (email: dkaushal@tulane.edu) or to S.M. (email: smehra@lsu.edu).

Despite widespread use of the bacille Calmette-Guérin (BCG) vaccine, *Mycobacterium tuberculosis* (*Mtb*) infection and the resulting incidence of tuberculosis (TB) remains a major global concern. The BCG vaccine, to a large extent and with some exceptions, mitigates only the most severe aspects of infection and exhibits a highly variable efficacy, especially in high-burden areas¹. The majority of *Mtb*-infected individuals, including BCG-vaccinated ones, develop persistent but asymptomatic TB infection following *Mtb* exposure, rather than sterilizing immunity². These individuals retain a finite risk of reactivation because of comorbidities such as HIV or diabetes. Developing new and efficacious TB vaccines is clearly the most effective intervention for containing the TB pandemic^{3–5}. To this end, a number of novel candidates are currently being evaluated either as potential replacements for BCG or to boost BCG-generated responses using a variety of approaches⁶. However, a frontline candidate that attempted to boost existing BCG responses failed to protect a target population against TB in a high-burden setting⁷. These results provide further impetus to the objective of replacing BCG with a new live attenuated vaccine.

The failure to generate an effective TB vaccine is attributed to a lack of specific immune correlates of protection from *Mtb* infection and TB disease. Of interest are adaptive responses, particularly pathogen-specific memory CD4⁺ and CD8⁺ T-cell-mediated responses essential for successful bacterial control during LTBI. BCG is generally considered to be inefficient in generating central memory CD4⁺ and CD8⁺ T-cell responses⁸, although long-term immunity following BCG administration is possible in some settings⁹. This contributes to the widely perceived inability of the vaccine to confer long-term protection against TB¹⁰. Thus, understanding related immune parameters and how perturbation by comorbidities leads to TB may be useful for effective TB vaccine design.

Aerosol delivery of BCG to the lung enhances protective efficacy¹¹, including in macaques¹². Further, aerosol TB vaccination might allow co-delivery of vaccine and adjuvants¹³. Aerosol-BCG resulted in significantly improved protection in guinea pigs against *Mtb* challenge compared with conventional vaccination¹¹. Besides, an adenoviral vector expressing *Mtb* antigens elicited robust responses following aerosol delivery¹⁴.

Attenuated mycobacteria have evoked interest as potential BCG-replacement vaccines¹⁵. The *Mtb* antigen repertoire counterintuitively evokes strong immunity, suggesting that such responses work in the pathogen's favour¹⁶. Immune-evasive pathways of *Mtb* are therefore the key to understand mechanisms of *Mtb* persistence¹⁷. SigH orchestrates a key stress-response pathway in *Mtb* that mitigates oxidative stress through induction of antioxidant production¹⁸. The *Mtb* mutant in *sigE*, which is part of the SigH regulon, elicited protection from *Mtb* infection¹⁹.

Further, the *M. avium paratuberculosis sigH* mutant is being evaluated as a candidate vaccine for protecting cattle (US20140271719A1 (Pending US Patent, Adel Talaat)). Besides, aerosol immunization of macaques with the *MtbΔsigH* mutant failed to cause disease²⁰. This was in direct contrast to the phenotype of this mutant in C57Bl/6 mice, in which the *sigH*-null strain replicated to levels comparable to those of parental *Mtb*¹⁸. While the *MtbΔsigH* mutant in H37Rv did not have a phenotype in monocytes²¹, the mutant in the CDC1551 strain exhibited growth restriction in bone marrow-derived macrophages (BMDMs)²². These results suggest that *MtbΔsigH* fails to neutralize host-generated oxidants *in vivo* and is controlled in an elite manner by the primate innate immune system. Macaques accurately model several aspects of the human TB syndrome including partial protection from BCG vaccination^{23,24}, different outcomes²⁵ and the full spectrum of pathology^{26,27}, and have the unique capacity to model *Mtb*/HIV co-infection^{28,29}. A World Health Organization working group strongly recommended validation of candidate live TB vaccines in this model³⁰.

In the current study, aerosol vaccination with *MtbΔsigH* elicited strong CD4⁺ and CD8⁺ central memory T-cell responses as well as a robust T-helper 1 (Th1) response correlating with significantly greater protection from lethal *Mtb* challenge in rhesus macaques. Furthermore, protection from lethal TB in *MtbΔsigH*-vaccinated animals was characterized by the presence of highly organized bronchus-associated lymphoid tissue (iBALT) associated with granulomas, following *Mtb* challenge.

Results

***MtbΔsigH* infection and increased iBALT.** We have previously established a correlation between the levels of ectopic lymphoid structures known as iBALT and the control of *Mtb* infection in a latent state. Experimentally infected macaques had significantly greater levels of iBALT in their lungs during LTBI, and this response was markedly reduced during TB disease³¹. iBALT was characterized by the presence of CD20⁺ B and CXCR5⁺ T cells. The expression of CXCR5 on T cells within iBALT follicles governed correct orientation and localization of T cells and macrophage activation³¹. Since aerosol infection of macaque lungs with *MtbΔsigH* resulted in the virtually complete clearance of infection, we used samples from this previous study²⁰ to assess whether the lungs of *MtbΔsigH*-infected macaques harboured increased iBALT. Lung sections from six macaques, each exposed to high doses of *Mtb* CDC1551 strain or the isogenic *MtbΔsigH* mutant, were co-stained for expression of CD3 and CD45R (B220)³¹. Immunofluorescence revealed that lung lesions from animals infected with the mutant contained significantly greater iBALT signal (Fig. 1a), relative to those infected with *Mtb*

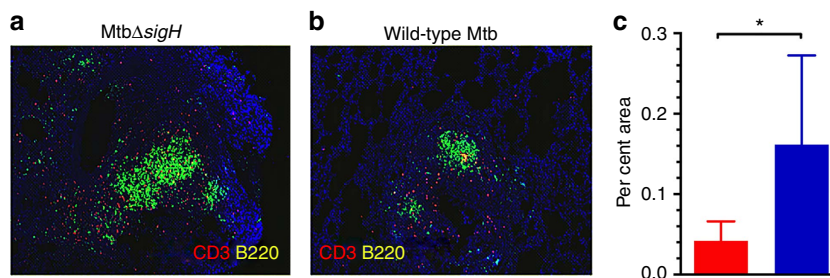


Figure 1 | iBALT formation induced by *MtbΔsigH* vaccination. Co-staining with CD3 and B220 revealed that lung granulomas following infection with *MtbΔsigH* (a) exhibited a significantly increased iBALT response relative to infection with *Mtb* (b). White scale bar, 500 μm. Data from multiple lesions from six different animals were used in the analyses. (c) The percentage of area occupied by iBALT follicles relative to total lung area was analysed in animals challenged with *Mtb* (red) and *MtbΔsigH* (dark blue). **P* < 0.05 (Student's *t*-test). Data are means ± s.d. Samples from four to five animals in each group were used for analysis.

(Fig. 1b). The percentage of area occupied by iBALT was significantly greater in samples from *MtbΔsigH*-infected than *Mtb*-infected animals ($P < 0.05$; Fig. 1c). In addition, the total lung area involved in iBALT follicles (μm^2 ; $P < 0.01$) and the average size of these iBALT follicles (μm^2 ; $P < 0.0001$, Student's *t*-test) was also significantly greater in sections derived from *MtbΔsigH*-infected, relative to *Mtb*-infected animals (Supplementary Fig. 1a,b). These results further support our previous observations that protection from *Mtb* infection directly correlates with the presence of granuloma-associated iBALT and suggested that the lungs of *MtbΔsigH*-infected macaques could exemplify an environment conducive to protection from TB.

Analysis of aerosol-*MtbΔsigH* as an anti-TB vaccine candidate.

Encouraged by the magnitude of iBALT induction in macaques infected with *MtbΔsigH*, we conceived a vaccine study to assess both the immunogenicity as well as the efficacy of this mutant as a potential vaccine against pulmonary TB. The design of the macaque study is outlined in Fig. 2a. Since enhanced iBALT responses were observed in the lungs of animals infected with the mutant strain via the aerosol route, we postulated that vaccination via the same route would have a greater chance of eliciting protection. Furthermore, BCG vaccination is more effective via the pulmonary route, indicating that local responses, elicited by matching the route of the vaccination to that of infection, may be critical to protect against TB^{11,12}. Before and following single aerosol vaccination with *MtbΔsigH* at a dose that elicited strong iBALT response²⁰, both peripheral blood and lung compartments were repeatedly sampled to obtain cells for immune studies and transcriptomics. Eight weeks post vaccination, animals were challenged via aerosol, with a highly lethal dose of *Mtb*. Unvaccinated and BCG (aerosol)-vaccinated groups were

included as appropriate controls (Fig. 2a). All animals that received aerosol-BCG or *MtbΔsigH* vaccination became tuberculin skin test (TST) positive (Supplementary Table 1).

Absence of disease on vaccination with *MtbΔsigH* or BCG.

Aerosolization of broth-cultured, log-phase BCG and *MtbΔsigH* was performed as described in the Methods section^{20,25,29,32,33}. Microbial efficiency of BCG and *MtbΔsigH* was highly equivalent during aerosolization. Aerosol vaccination of macaques with *MtbΔsigH* and BCG deposited $\sim 1,000$ colony-forming unit (CFU) bacilli into the deep lung. Aerosol vaccination with either strain resulted in a positive TST (Supplementary Table 1) but did not induce dyspnoea, anorexia or significant changes in body temperatures relative to pre-infection values (Fig. 2b). The body weights of all vaccinated animals also remained relatively normal during the post-vaccination/pre-challenge phase with the exception of a slight decline ($< 3\%$) in the body weights of BCG-vaccinated animals 3–4 weeks post vaccination (Fig. 2c). None of the vaccinated animals exhibited an increase in serum C-reactive protein (CRP) levels relative to unvaccinated animals at any time post vaccination (Fig. 2d). Further, thoracic radiographs acquired post vaccination on all 14 vaccinated animals were normal (Fig. 2e).

Differential persistence of *MtbΔsigH* and BCG in BAL.

The persistence of live mycobacteria was evaluated in bronchoalveolar lavage (BAL) from both *MtbΔsigH*- and BCG-vaccinated macaques. Three weeks after vaccination, greater levels of *MtbΔsigH* were recovered from BAL compared with BCG (Fig. 3a). At week 5 post vaccination, BCG could not be recovered from BAL, while detectable levels of *MtbΔsigH* were still recovered (Fig. 3a), indicating that this strain might persist longer

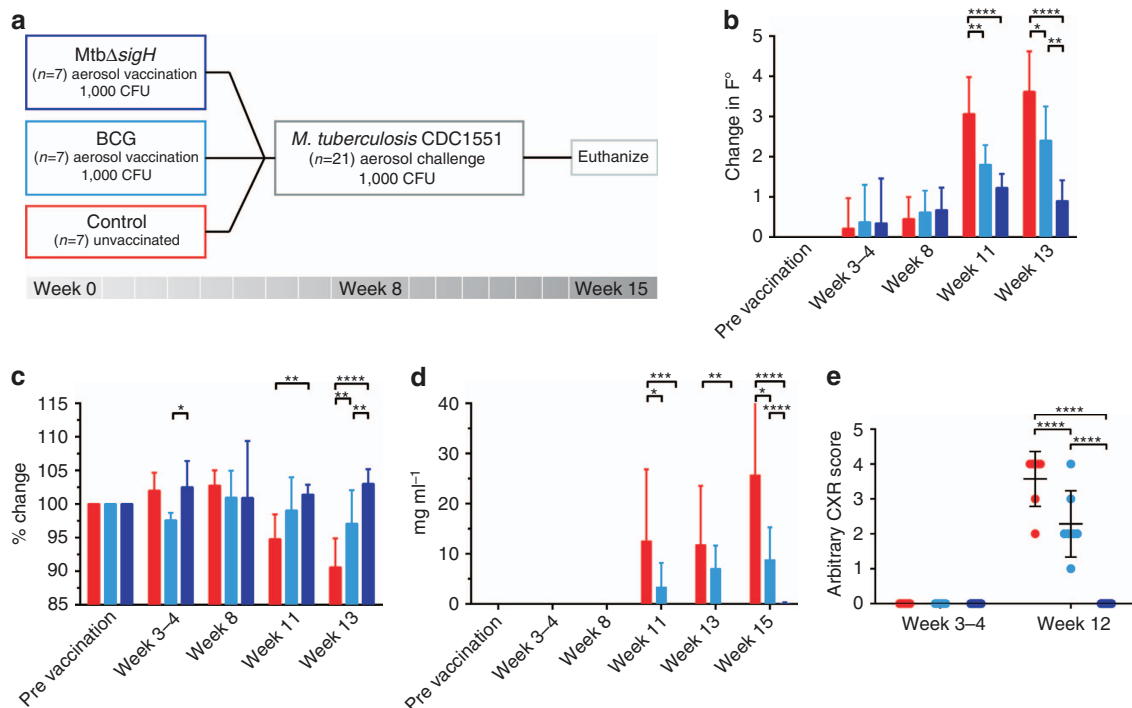


Figure 2 | Study outline and clinical correlates of vaccination and infection. (a) Three groups of seven macaques were used: unvaccinated (red); vaccinated with BCG (light blue) and vaccinated with *MtbΔsigH* (dark blue). (b) Changes ($\Delta^{\circ}\text{F}$) in body temperature; (c) changes in percentage of body weight; (d) changes in serum CRP ($\mu\text{g ml}^{-1}$) levels; and (e) changes in relative thoracic radiograph (CXR) scores, over the course of the vaccination and infection phases. CXRs were scored in a blinded manner by categorizing between zero and four based on increasing involvement in the granulomatous pathology. $*P < 0.05$, $**P < 0.01$, $***P < 0.001$, $****P < 0.0001$ using two-way ANOVA with Tukey's correction for multiple comparisons. Data are means \pm s.d. Samples from all seven animals in each group were used for analysis at each time point.

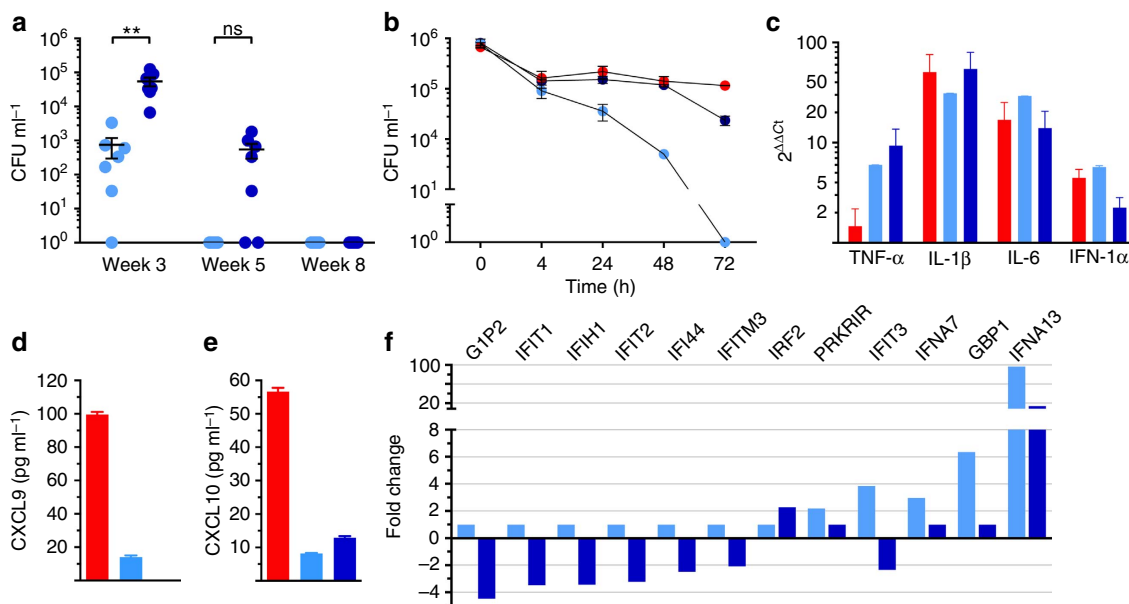


Figure 3 | Comparative measures of bacterial burden in BAL following aerosol vaccination and restriction during intraphagosomal culturing *in vitro*. (a) BCG (light blue) and MtbΔsigH (dark blue) CFU levels in total BAL samples at weeks 3, 5 and 8 after vaccination. (b) Rhesus macaque BMDM *in vitro* killing assay in CFU ml⁻¹ with *Mtb* (red), BCG and MtbΔsigH. ***P* < 0.01 using two-way ANOVA with Tukey's correction for multiple comparisons. Data are means ± s.d. (c) Relative expression (2^{ΔΔCt}) of TNF-α, IL-1β, IL-6 and IFN-1α in BMDMs infected with *Mtb*, BCG and MtbΔsigH using real-time RT-PCR. (d, e) Absolute expression of CXCL9 (d) and CXCL10 (e; pg ml⁻¹) in supernatants derived from BMDMs infected with *Mtb*, BCG and MtbΔsigH using cytokine analysis assay. (f) Microarray-derived fold changes of gene expression of 12 Type I interferon genes in the BAL of BCG- and MtbΔsigH-vaccinated animals. For analysis involving BAL, samples from all seven animals in each group were used for analysis at each time point (a). For CFU analysis *in vitro*, the experiment was performed twice, with four biological replicates in each instance (b). Transcript and cytokine analyses were performed on biological replicates (c-f). ns, not significant.

than BCG in human lungs. Eight weeks after vaccination, CFU for neither strain was recovered from the BAL of vaccinated macaques. Furthermore, macaque BMDMs were able to kill BCG at a faster rate than both *Mtb* and MtbΔsigH *in vitro* (Fig. 3b). BMDMs infected with MtbΔsigH expressed greater levels of tumour-necrosis factor-α (TNF-α) and interleukin (IL)-1β but not IL-6 transcripts relative to BCG (Fig. 3c). In addition, BMDMs infected with MtbΔsigH also secreted significantly lower levels of inflammatory chemokines CXCL9 (Fig. 3d) and CXCL10 (Fig. 3e) in supernatants, relative to the BCG-vaccinated or the unvaccinated groups. Both the expression and anti-*Mtb* activity of TNF-α is strongly enhanced by IL-1β via direct augmentation of caspase-dependent apoptosis³⁴. Infection of BMDMs with MtbΔsigH results in both higher TNF-α expression and greater apoptosis relative to *Mtb*²². The activity of IL-1β is itself regulated by Type I interferons, whose expression is positively controlled by IRF1 and negatively by IRF2. Elicitation of Type I interferon response inhibits IL-1β and TNF-α activity, and promotes the progression of active TB, as is the case during infection with hypervirulent *Mtb* strains³⁵. Abrogation of Type I responses reverses this trend and is being considered as a host-directed therapy for TB³⁶. Accordingly, the expression of Type I genes was significantly higher in BAL samples obtained 3 weeks after vaccination from animals that received BCG, and significantly lower in animals that received MtbΔsigH (Fig. 3f). The IRF2 gene expression level was lower in the BAL of BCG-vaccinated and more than twofold higher in the BAL of MtbΔsigH-vaccinated animals (Fig. 3f). The expression of prototypical Type I molecule IFN-γ was also higher in BMDMs infected with BCG and *Mtb*, relative to those infected with MtbΔsigH (Fig. 3c).

MtbΔsigH induces protective immune signatures in the lung. Global immune responses to vaccination with MtbΔsigH or BCG

were analysed by transcriptome profiling of BAL samples collected before vaccination and 3 weeks post vaccination. The genes significantly induced in BAL after BCG vaccination were involved in cellular transport, DNA binding by regulatory protein, RNA processing or were part of the lumen, non-membrane-bound organelle or macromolecular complex assembly (Fig. 4). The only major category of genes induced following BCG vaccination was that categorized as pertaining to immune system development (Fig. 4). Conversely, the expression of genes involved in NK cell signalling, MAPK signalling and JAK/STAT signalling, cytokine signalling, T-cell signalling, calcium signalling, neuroactive/growth receptors and lipid biosynthesis were induced to higher levels in the BAL from MtbΔsigH-vaccinated macaques (Fig. 4). Further, a large majority of these genes were either not expressed or were expressed to significantly lower levels in the BAL of animals vaccinated with BCG (Fig. 4). Thus, vaccination with MtbΔsigH appeared to result in the induction of a markedly stronger innate immune response, as indicated by the differential induction of NK cell, MAPK and JAK/STAT signalling pathways as well as genes from the cytokine, T-cell receptor and calcium signalling pathways (Fig. 4), although the differential persistence of the two mycobacterial strains could have played a role in this differential response. In addition, enhanced immune cell differentiation, proliferation, activation and processing, as well as macromolecular synthesis, which are associated with heightened cytokine and T-cell responses, were evidenced by the increased expression levels of neuroactive/growth factor receptor signalling, potentiation and lipid biosynthesis pathways in BAL samples derived from animals vaccinated with MtbΔsigH (Fig. 4).

Local increases in T cells due to MtbΔsigH vaccination. Local and systemic immune responses were compared following vaccination by analysis of BAL and blood, respectively. Marked

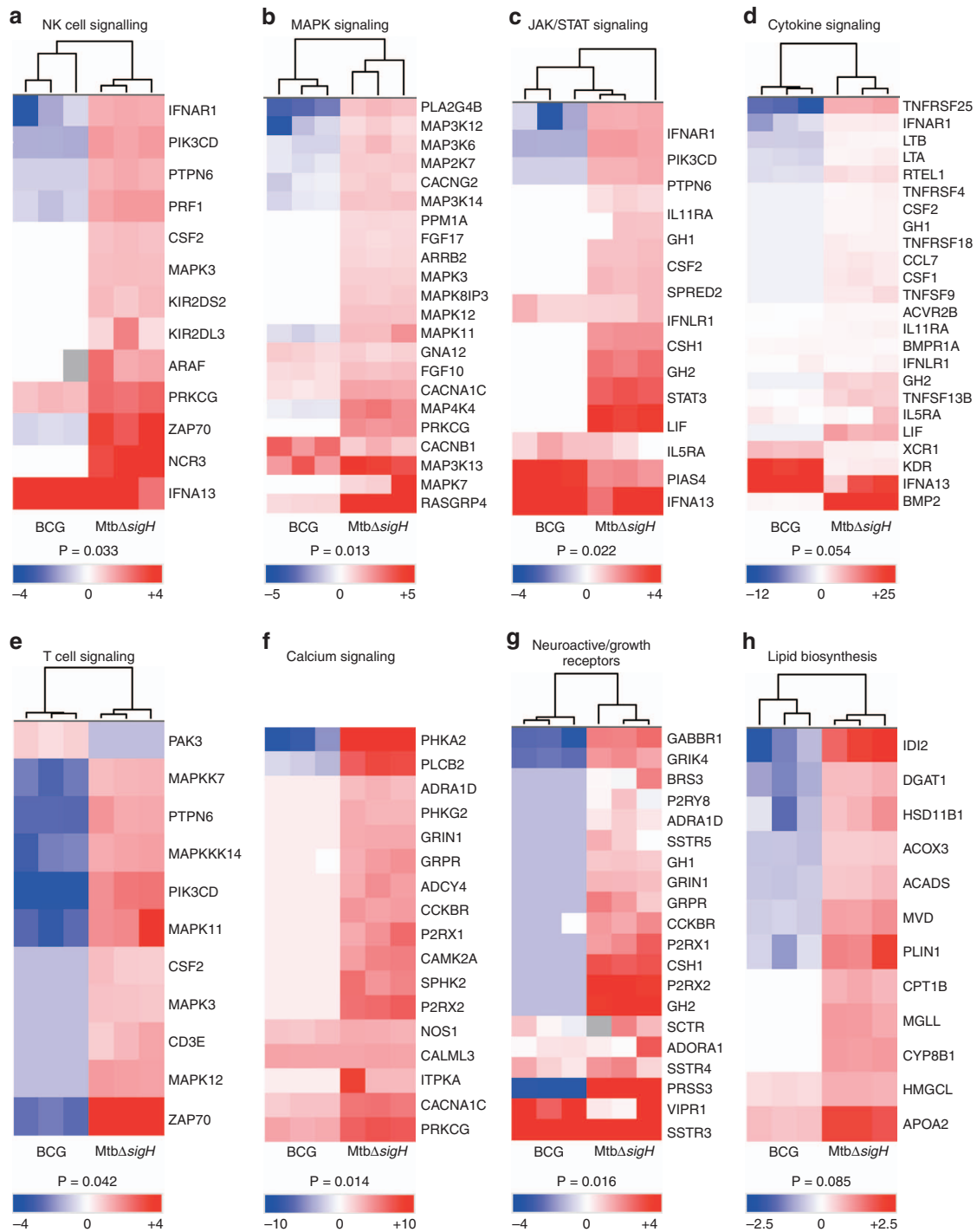


Figure 4 | Transcriptomics from BAL 3 weeks after immunization. Total RNA isolated from BAL samples of three animals vaccinated with BCG and another three with *MtbΔsigH*, obtained 3 weeks after vaccination, was subjected to amplification and macaque-specific DNA microarray analysis. The expression of genes belonging to natural killer cells (a), MAP Kinase (b), JAK/STAT (c), cytokine (d), T cells (e), calcium signalling (f), neuroactive/growth receptors (g) and lipid biosynthesis (h) pathways were induced to significantly higher levels in the BAL of animals vaccinated with *MtbΔsigH*, relative to those vaccinated with BCG. *P* values shown are derived from the analysis of significant terms in DAVID with Bonferroni correction for multiple comparisons. BAL samples from three animals in each group were used for microarray experiments.

increases in CD4⁺ and CD8⁺ T-cell numbers were found in BAL immediately post vaccination ($P < 0.001$; two-way analysis of variance analysis of variance (ANOVA) with Tukey’s correction; Fig. 5a,b); however, no differences in the frequency of CD4⁺ and CD8⁺ T cells were observed in the periphery post vaccination (Supplementary Fig. 2). In addition, no differences in the chemokine receptors CXCR3, CXCR4, CCR7 or activation

marker CD69 were detected systemically, which indicated no significant variation in the functional phenotype of T cells in the blood (Supplementary Fig. 3). However, a significant increase in the number of circulating CD4⁺CCR5⁺ T cells was discovered in the *MtbΔsigH* group between weeks 2 and 3 ($P < 0.05$; two-way ANOVA with Tukey’s correction; Supplementary Fig. 3). No differences were observed in the memory status of circulating

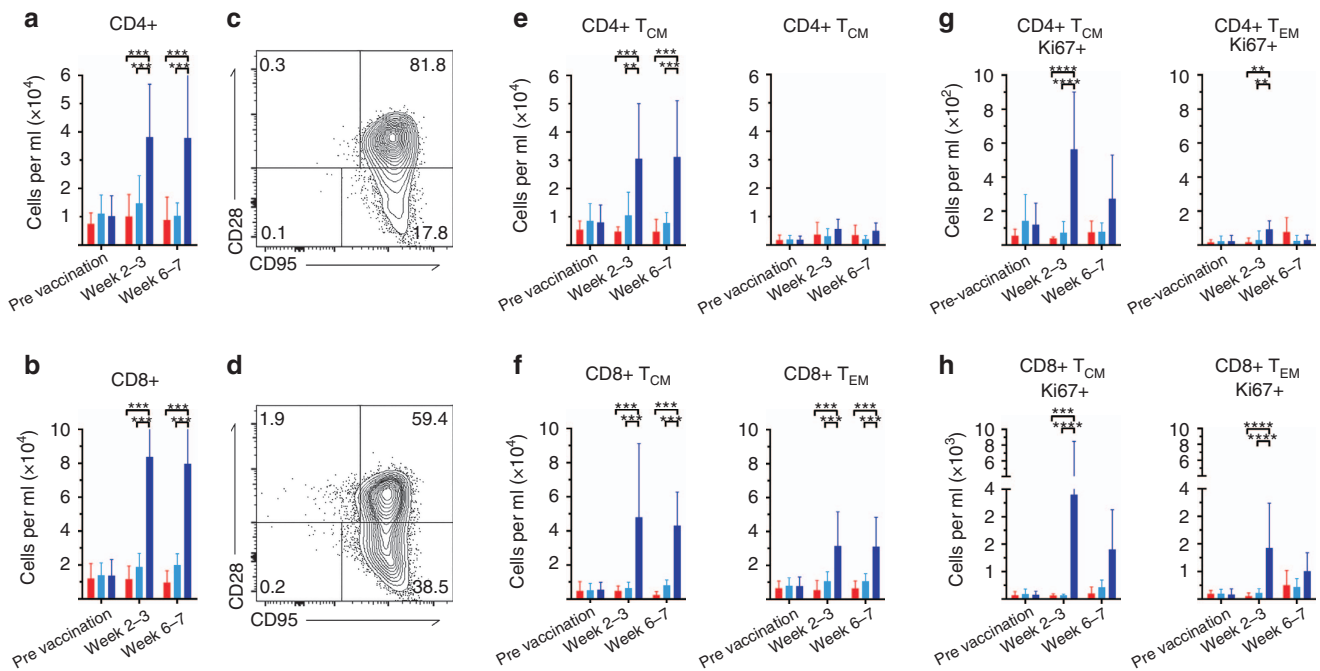


Figure 5 | T-cell response to immunization in BAL. Vaccination with *MtbΔsigH* (dark blue) induced a significantly higher central memory immune response relative to BCG vaccination (light blue), or no vaccination (red). Quantification of CD4⁺ (a) and CD8⁺ (b) T cells migrating to the lung after vaccination. Representative plots of central memory (CD28⁺CD95⁺), effector memory (CD28⁻CD95⁺) and naïve (CD28⁺CD95⁻) CD4⁺ (c,e) and CD8⁺ (d,f) T cells in BAL. Quantification of CD4⁺ (e) T_{CM} and T_{EM} cells, CD8⁺ T_{CM} and T_{EM} cells (f) in BAL, and the proliferative capability of these cells (g,h). **P*<0.05; ***P*<0.01; ****P*<0.001; *****P*<0.0001 using two-way ANOVA with Tukey's correction for multiple comparisons. Data are means ± s.d. BAL samples from all 21 animals (*n* = 7, three groups) were included in the flow cytometry experiments and analyses. Samples from all seven animals in each group were used for analysis at each time point.

T cells, including central (T_{CM}-CD28⁺CD95⁺) and effector memory (T_{EM}-CD28⁻CD95⁺) cells or naïve T cells (CD28⁺CD95⁻; Supplementary Fig. 2)³⁷.

While no significant changes were discovered in T-cell frequencies in the peripheral blood, a strong lung-specific central and effector memory response was initiated post vaccination with *MtbΔsigH*. This response was apparent immediately after vaccination by significant increases in the number of CD4⁺ central memory (T_{CM}) (*P*<0.01–0.001; two-way ANOVA with Tukey's correction) as well as CD8⁺ T_{CM} and effector memory (T_{EM}; *P*<0.001) in the BAL (Fig. 5c–f), with a marked increase in proliferation as measured by Ki67 positivity (*P*<0.01–0.0001; Fig. 5g,h). A significant increase in the number of CD69⁺ T cells (*P*<0.001 for *MtbΔsigH* versus BCG and *P*<0.01–0.001 for *MtbΔsigH* versus unvaccinated groups; Fig. 6a,b) indicated that T cells in BAL were antigen-stimulated via the T-cell receptor. The polarity of the T-cell response was examined using the markers CCR5 and CXCR3, which are preferentially expressed by Th1 cells, as well as CXCR4, which is preferentially expressed by T-helper 2 (Th2) cells. The results revealed that T cells in BAL immediately post-*MtbΔsigH* vaccination preferentially expressed high levels of CCR5 and CXCR3 compared with T cells recruited following vaccination with BCG (*P*<0.01–0.001; Fig. 6c,d). Thus, aerosol vaccination with *MtbΔsigH* induced transcriptomic and cellular signatures indicative of a strong Th1 response that resulted in accumulation of memory T cells.

Vaccination with *MtbΔsigH* protects from lethal *Mtb* challenge.

To evaluate the potential of the attenuated mycobacterium to serve as a TB vaccine, all animals were challenged with a high dose of *Mtb* CDC1551, which has historically produced lethal TB in rhesus macaques within 10 weeks^{20,32}. Unvaccinated animals

rapidly developed pulmonary granulomatous pathology with rapid increases in body temperatures (*P*<0.01 for *MtbΔsigH* relative to BCG and *P*<0.0001 for *MtbΔsigH* versus unvaccinated groups; two-way ANOVA with Tukey's correction) and serum CRP levels (*P*<0.0001 for *MtbΔsigH* versus both other groups; Fig. 2b,d), as well as a swift decline in body weights *P*<0.01 for *MtbΔsigH* relative to BCG and *P*<0.0001 for *MtbΔsigH* versus unvaccinated groups; Fig. 2c). Control animals also exhibited high levels of pulmonary granulomatous involvement by radiology (Fig. 2e). The same clinical measure also increased, albeit to a lesser degree, in animals that were aerosol-vaccinated with BCG, while animals vaccinated with *MtbΔsigH* exhibited virtually no evidence of disease (*P*<0.0001 for *MtbΔsigH* versus unvaccinated as well as versus BCG; Fig. 2b–e). Three weeks post-*Mtb* challenge (week 11), the increase in body temperatures in unvaccinated animals was significant relative to BCG-vaccinated (*P*<0.01) and highly significant relative to *MtbΔsigH*-vaccinated animals (*P*<0.0001; two-way ANOVA with Tukey's correction; Fig. 2b). Five weeks post challenge (week 13), the differences in body temperature between the unvaccinated and BCG-vaccinated groups were significant (*P*<0.05); the differences between the BCG and *MtbΔsigH*-vaccinated groups were very significant (*P*<0.01); and the differences between the unvaccinated and *MtbΔsigH*-vaccinated groups were highly significant (*P*<0.0001; Fig. 2b). The differences in body weight between the unvaccinated and *MtbΔsigH*-vaccinated groups and the BCG and *MtbΔsigH*-vaccinated groups were very significant at week 11 (*P*<0.01; Fig. 2c) and while by week 13, these differences had become highly significant (*P*<0.0001; two-way ANOVA with Tukey's correction). Profoundly lower serum CRP levels were detected in the macaques vaccinated with *MtbΔsigH* relative to macaques that were not vaccinated at weeks 11 and 13 and at time of euthanasia (*P*<0.0001). At both week 11 (*P*<0.05) and

while euthanasia ($P < 0.0001$; two-way ANOVA with Tukey's correction), the serum CRP levels detected in the macaques vaccinated with *MtbΔsigH* were also significantly lower than levels measured in the BCG-vaccinated group (Fig. 2d). Similarly, animals vaccinated with *MtbΔsigH* exhibited significantly lower chest X-ray (CXR) scores, consistent with lack of disease following lethal challenge, in this group, relative to either BCG-vaccinated or unvaccinated macaques ($P < 0.0001$ in both cases).

While extensive pathology was not discernable in the lungs of macaques vaccinated with the mutant, a majority of those vaccinated with BCG exhibited moderate CXR scores, again significantly lower than those in the unvaccinated group, where pathology consistent with military TB could be observed in a majority of animals.

Vaccination with *MtbΔsigH* reduces *in vivo* bacterial burdens.

The protection conferred by *MtbΔsigH* was also evident following evaluation of bacterial burdens. Significantly lower *Mtb* was recovered from BAL from *MtbΔsigH*-vaccinated animals relative to those vaccinated with BCG at 3 and 5 weeks after challenge (weeks 11 and 13; Fig. 7a). At the time of euthanasia, the total lung burden in animals vaccinated with *MtbΔsigH* was three logs lower than burdens in unvaccinated ($P < 0.01$) and two logs lower than burdens in BCG-vaccinated ($P < 0.01$) animals, while bacterial loads in animals vaccinated with BCG were only 0.5–1 logs lower than in the control group ($P < 0.05$; one-way ANOVA with Tukey's correction; Fig. 7b). We were unable to culture *Mtb* from >42% of all lung sections obtained from macaques vaccinated with *MtbΔsigH*. In contrast, every section obtained from either unvaccinated animals or those vaccinated with BCG was positive for *Mtb*. Thus, the *Mtb* burden was significantly lower in the lungs of *MtbΔsigH*-vaccinated animals following lethal challenge compared with those vaccinated with BCG. Similar results were obtained when bronchial lymph node bacterial burdens were analysed at necropsy (Fig. 7c). Using a combination of hygromycin resistance/sensitivity and PCR, we verified that the obtained CFUs were *Mtb* and not residual *MtbΔsigH* or BCG.

Vaccination with *MtbΔsigH* leads to reduced lung pathology.

The results of the pulmonary pathology analyses mirrored those obtained following analysis of bacterial burdens. Animals vaccinated with *MtbΔsigH* exhibited significantly fewer pulmonary lesions on challenge, as determined by both gross and histopathological examination (Fig. 8a–f and Supplementary Fig. 4) and morphometric quantitation (Fig. 8g). Thus, the animals vaccinated with *MtbΔsigH* had fewer granulomas (the extent of lung affected by TB lesions following *Mtb* infection encompassed an average of 4%), and less TB-related pathology (for example, oedema, pneumonia and generalized foci of inflammation) than animals in the other two groups (where ~40% of the lung was affected; $P < 0.0001$ in both cases; one-way ANOVA with Tukey's correction; Fig. 8g). The clinical and microbiological differences also correlated with significant differences in overall survival rates following challenge (Fig. 8h). All seven unvaccinated animals succumbed to massive pulmonary TB following a lethal aerosol *Mtb* challenge within a median of 36 days. Five out of seven BCG-vaccinated animals also succumbed to TB, within a median of 48 days. None of the *MtbΔsigH*-vaccinated animals exhibited any overt signs of disease or required euthanasia (Fig. 8h).

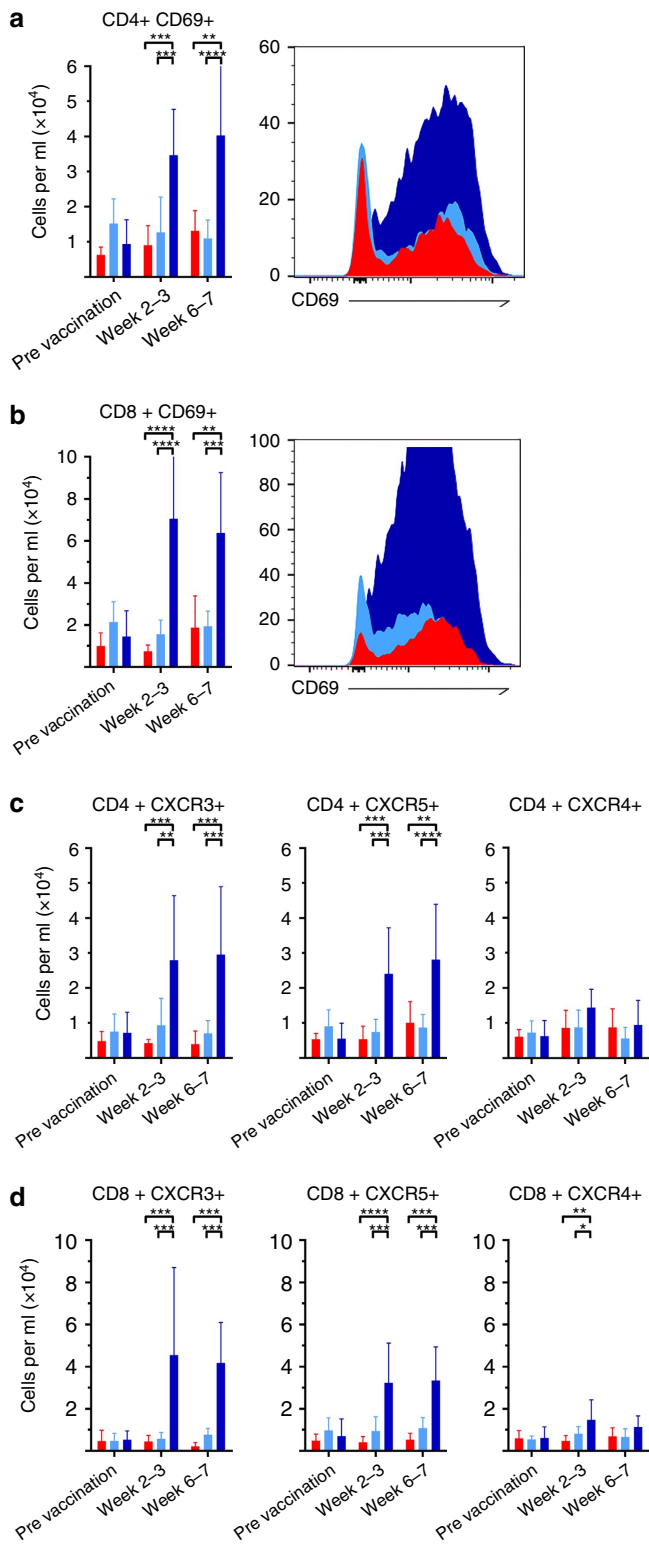


Figure 6 | Local T-cell phenotype to immunization in BAL. Vaccination with *MtbΔsigH* (dark blue) induced a significantly stronger T_{H1} cell response relative to BCG vaccination (light blue), or no vaccination (red). Quantification of and representative histograms of CD4⁺CD69⁺ (a) and CD8⁺CD69⁺ (b) T cells migrating to the lung after vaccination. Absolute cell counts of phenotypic markers CXCR3, CCR5 and CXCR4 in CD4⁺ (c) and CD8⁺ (d) T cells in BAL at different stages of infection. * $P < 0.05$, ** $P < 0.01$, *** $P < 0.001$, **** $P < 0.0001$ using two-way ANOVA with Tukey's correction for multiple comparisons. Data are means \pm s.d. BAL samples from all 21 animals ($n = 7$, three groups) were included in the flow cytometry experiments and analyses. Samples from all seven animals in each group were used for analysis at each time point.

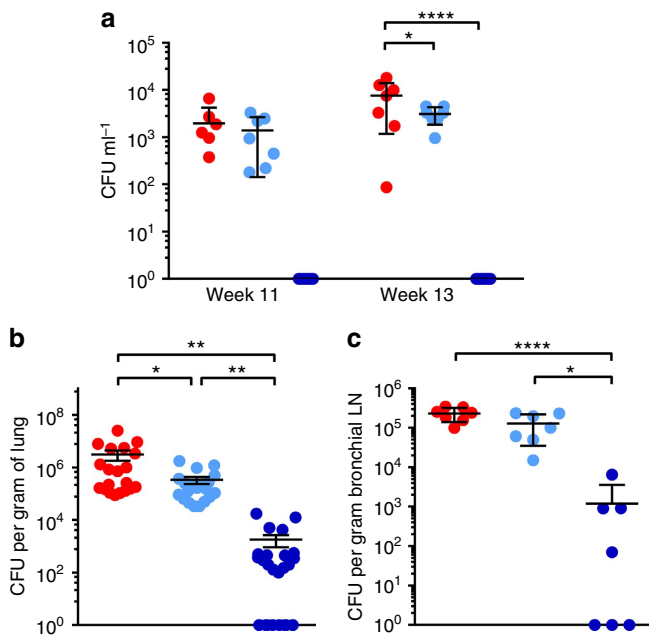


Figure 7 | Bacterial burden following lethal *Mtb* challenge. (a) *Mtb* CFU levels in total BAL samples at week 11 (3 weeks after challenge) and week 13 (5 weeks after challenge); (b) *Mtb* levels per gram of lung tissue at necropsy (c) *Mtb* burdens per gram of bronchial lymph node tissue at * $P < 0.05$; ** $P < 0.01$; *** $P < 0.001$; **** $P < 0.0001$, (a) two-way ANOVA and (b,c) one-way ANOVA with Tukey's multiple testing correction. Data are means \pm s.d. Samples from all seven animals in each group were used for analysis at each time point. For analysis of lung burdens, four pooled samples (two each from left and right lung) from each macaque, each representing five distinct lung sections were used (b). For analysis of bronchial lymph node burdens, one section from each animal was analysed.

Differential T-cell responses in animals post challenge. To assess an immunologic basis for protection induced by *MtbΔsigH*, the functional phenotype of circulating $CD4^+$ and $CD8^+$ T cells was analysed by employing the same markers used for evaluating pulmonary responses following vaccination. No significant differences in the percentages of $CD4^+$ and $CD8^+$ central or effector memory cells were observed in peripheral blood immediately following challenge (Supplementary Fig. 2). However, a significant increase in $CD4^+$ $CCR5^+$ T cells was identified 7 weeks after *Mtb* challenge, as well as a significant decrease in $CD8^+$ $CXCR3^+$ T cells in peripheral blood at weeks 3 and 7 following challenge in unvaccinated animals (Supplementary Fig. 3).

Consistent with overall lung involvement and chest radiograph scores, a significantly greater number of $CD4^+$ and $CD8^+$ T cells including T_{CM} and T_{EM} were present in BAL in the unvaccinated animals compared with both BCG and *MtbΔsigH*-vaccinated animals (Fig. 9a–d). The increased numbers of T cells in BAL in unvaccinated animals were also evident from representative histograms of $CD69^+$ T cells (Supplementary Fig. 5a,b). While no significant differences were observed in $CXCR3$, $CCR5$ and $CXCR4$ expression by $CD4^+$ or $CD8^+$ T cells between the two vaccinated groups (Supplementary Fig. 5c,d), a significant decrease in the number of $CD8^+$ $CXCR4^+$ was noted at weeks 11 and 15 in the *MtbΔsigH*-vaccinated group compared with the other two groups (Supplementary Fig. 5d).

Comparison of polyfunctional *Mtb*-specific T-cell responses. To examine antigen-specific responses to *Mtb*, isolated peripheral

blood mononuclear cells (PBMCs) collected 5 weeks post challenge were stimulated with whole *Mtb* cell wall and cell filtrate protein, and responses were analysed using intracellular cytokine staining for $IFN-\gamma$, IL-2 and $TNF-\alpha$. The results indicated that vaccination with *MtbΔsigH* and BCG correlated with significant increases in the percentage of polyfunctional, $IFN-\gamma^+$, $IL-2^+$, $TNF-\alpha^+$ $CD4^+$ T cells, whereas unvaccinated animals displayed a significantly greater number percentage of monofunctional $CD4^+$ T cells (Fig. 9e,f). Unfortunately, samples from other time points were not available for analysis.

Profound iBALT post challenge in *MtbΔsigH*-vaccinated animals.

Lung samples collected after lethal *Mtb* challenge from unvaccinated (Fig. 10a,d), BCG-vaccinated (Fig. 10b,e) and *MtbΔsigH*-vaccinated (Fig. 10c,f) macaques at the time of necropsy were assayed for iBALT by histopathology and immunofluorescence with CD3 and CD20 followed by confocal microscopy and image analysis. We observed that protection in each of these groups of macaques was strongly associated with levels of iBALT. Thus, the few, small granulomas in the lungs of animals vaccinated with *MtbΔsigH* and challenged with *Mtb* were characterized by the presence of multiple well-organized iBALT per lesion (Fig. 10c). The presence of the follicles was also apparent in the cognate haematoxylin and eosin stains (Fig. 10 c,f). These follicles were, in general, associated with granulomas and appeared to be an outgrowth of the outer lymphocyte-rich layer (Fig. 10 c,f). While B cells constituted the majority in these follicles, $CD3^+$ cells were also present (Fig. 10c). In contrast to the multiple well-developed iBALT associated with granulomas in *MtbΔsigH*-immunized animal, animals from the other groups (Fig. 10a,b,d,e) had fewer iBALT that were less well organized. The total area of iBALT in *MtbΔsigH*-vaccinated macaques was significantly greater after *Mtb* challenge (Fig. 10g) than in either of the other groups, despite the fact that the area occupied by granulomas in the *MtbΔsigH*-vaccinated group was significantly less compared with the other two groups after *Mtb* challenge (Fig. 10h). This further emphasizes the difference in BALT induction and the correlation between iBALT and latent control of *Mtb* infection.

Discussion

Previously, we showed that aerosolization of a high dose of *MtbΔsigH* into the lungs of rhesus macaques resulted in nonpathogenic infection²⁰. Here we demonstrate that pulmonary vaccination with this mutant protected against lethal challenge in macaques via the induction of a potent memory T-cell response. Further, we establish a strong correlation between the latent control of infection and iBALT, suggesting that these lymphoid structures facilitate control of TB by maintaining LTBI or sterilizing infection. Induction of BALT in response to respiratory infections is known to not only result in protection, but such responses are also less pathologic³⁸. Secondary T_{FH} cells, which constitute the great majority of lymphoid follicle (including iBALT) T cells, expand from memory T cells in a B-cell-aided manner³⁹. Our results therefore suggest that the interplay between B and T cells is critical for the proper development of granulomatous-protective responses to TB. This study substantiates previous work using the macaque model of TB, which showed that B cells produced antibody and were important for control of TB⁴⁰. Our results suggest that future studies should unravel the function of B cells recruited to the lung to understand immunity from TB.

While the correlates of vaccine-induced protective immunity against TB are not completely understood, T lymphocytes expressing markers of central memory response (dual positivity for $CD28$ and $CD95$)³⁷ are critical for protection. A model of

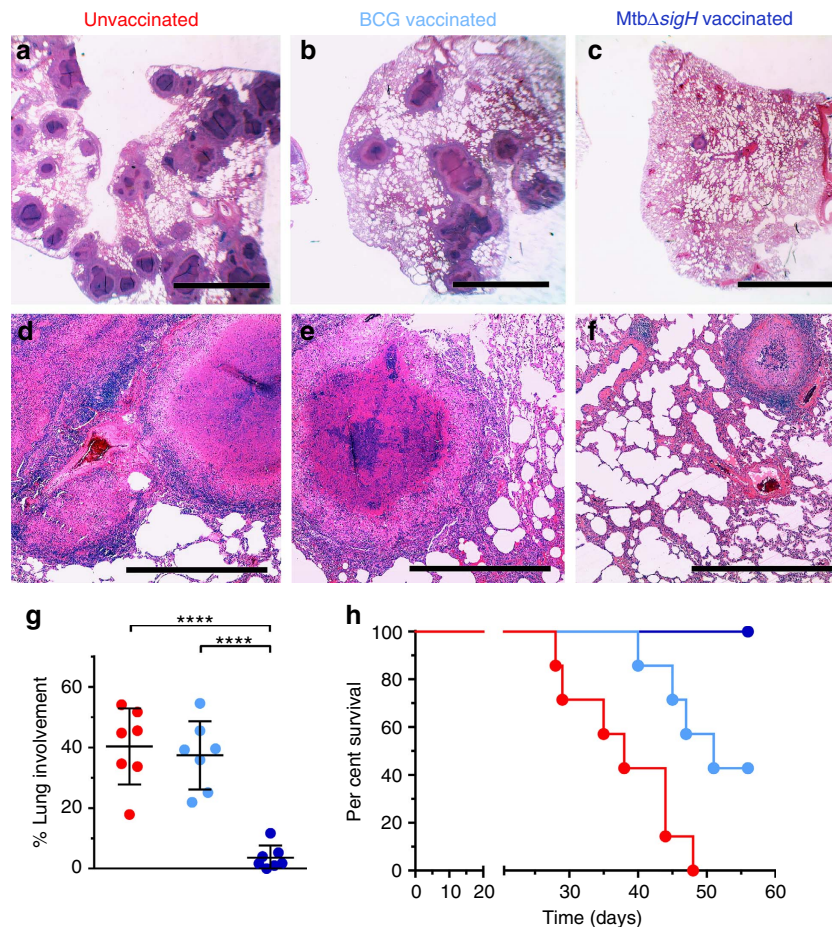


Figure 8 | Histopathological and survival analysis of lungs of *Mtb*-infected animals. Haematoxylin and eosin (H&E) staining from representative animals in each of the three groups. **(a,d)** Vaccine-naive group with miliary, white 2–4 mm granulomas and scattered lobular multicoloured areas of consolidation. **(b,e)** BCG-vaccinated with localized dark red lobar pneumonia and **(c,f)** *Mtb Δ sigH*-vaccinated with no apparent gross lesions. Black scale bars in **(a–c)**, 5 mm and **(d–f)**, 500 μ m. **(g)** Morphometric measures of pulmonary pathology in the different groups of unvaccinated (red), BCG-vaccinated (light blue) and *Mtb Δ sigH*-vaccinated (dark blue) animals. **** $P < 0.0001$ with **(g)** one-way ANOVA using Tukey's multiple testing correction. Data are means \pm s.d. **(h)** Survival proportion Kaplan-Meier curves for the three groups of animals, using Mantel-Cox (log-rank) survival analysis. At least three systematic random microscopic fields from each lung, representing most lung lobes, from each of the animals in every group were used for morphometric analysis **(g)**. Data from each of the seven animals per group was used for survival proportions analysis **(h)**.

protective immunity that is currently gaining credence suggests that initial vaccination(s) resulting in a spike in effector response can result in the establishment of a central memory response, which is likely to result in long-term protection⁴¹. T_{CM} are extremely proliferative and can rapidly evolve into large numbers of effector cells expressing high levels of pro-inflammatory cytokines (for example, $IFN-\gamma$). Consequently, the finding that pulmonary vaccination with *Mtb Δ sigH* resulted in potent T_{CM} (as well as T_{EM} , particularly $CD8^+$) responses during the post-vaccination phase that corresponded to a strong T_{EM} response in the challenge phase merits further evaluation. The role of chemokine receptors, including CXCR3, is critical to the recruitment of $CD8^+$ T cells, and CXCR3 expression on T_{CM} is strongly correlated with effective anti-pathogen memory responses⁴². BAL transcriptome profiling results indicated that animals vaccinated with *Mtb Δ sigH* developed a highly productive pulmonary immune response, both in terms of magnitude and breadth. Prior studies have established that $CD4^+$ T cells with specificity for mycobacterial antigens are critical for the control of *Mtb* infection⁴³, and that $CD8^+$ T cells play an increasingly important role in this process^{41,44}. SigH induces pathogen antioxidant responses during stress^{45,46}. *Mtb Δ sigH* is unable to induce expression of the transcriptionally linked thioredoxins and

thiol peroxidases⁴⁵ that act as antioxidant buffers against the host oxidative burst⁴⁷. Consequently, the antioxidant response of the *Mtb Δ sigH* mutant was strongly crippled⁴⁷, and the resulting production of oxidants likely enhanced antigen-specific $CD8^+$ T-cell responses through the cross-priming of antigen presentation⁴⁸. In addition, the ability of *Mtb Δ sigH* to persist longer than BCG allowed for increased stimulation and antigen presentation, inducing a stronger, more robust, T-cell repertoire⁴⁹. Further characterization of this T_{CM} response is however necessary to substantiate that these cells are not long-lived T_{EM} cells, since *Mtb Δ sigH* antigens persist longer than BCG.

The ability of aerosol *Mtb Δ sigH* vaccination to elicit highly protective responses in macaques could have roots in the fundamental processes that govern *Mtb*–macrophage interactions. *In vitro*, macrophages infected with this mutant elicited greater expression of Th1 pro-inflammatory cytokines $TNF-\alpha$ and $IL-1\beta$, and lower Type I interferon, relative to those infected with *Mtb* and BCG (this study and ref. 22). Together, these results indicate that the interaction of *Mtb Δ sigH* with host phagocytes is critically altered by the loss of the bacillus's ability to induce SigH-mediated antioxidant functions, relative to BCG. TNF can restrict macrophage-contained *Mtb* by several mechanisms, including by potently inducing early inflammatory responses⁵⁰,

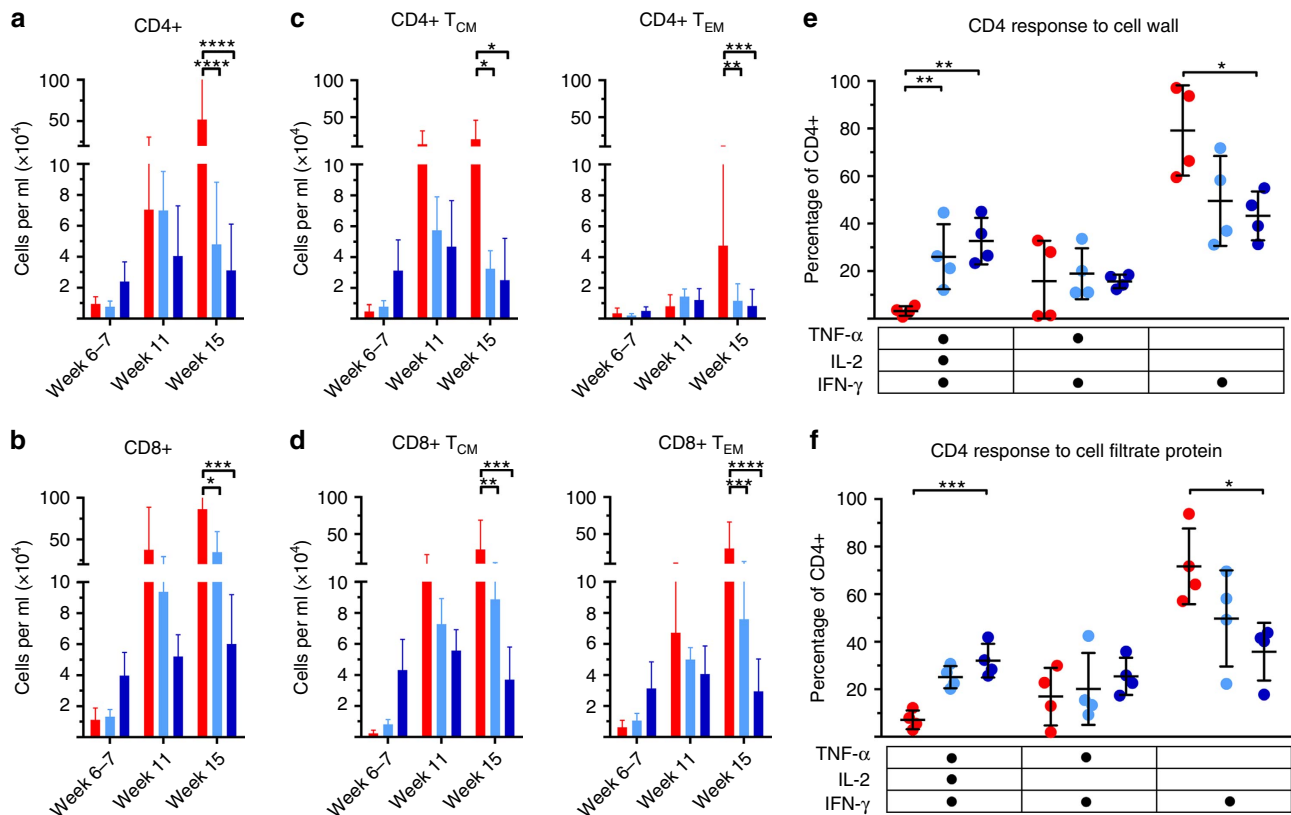


Figure 9 | Immune responses in the lung post-*Mtb* challenge. (a,b) Quantification of cells per ml of BAL of (a) CD4⁺ and (b) CD8⁺ T cells and of (c) CD4⁺ T_{CM} and T_{EM} cells and of (d) CD8⁺ T_{CM} and T_{EM} cells migrating to the lung after challenge in groups of unvaccinated (red), BCG-vaccinated (light blue) and *Mtb* Δ *sigH*-vaccinated (dark blue) animals. (e,f) Percentage of CD4⁺ T cells from PBMCs prepared from whole blood, producing gamma interferon, interleukin 2 and tumour necrosis factor alpha in response to (e) the *Mtb* cell wall and to (f) *Mtb* cell filtrate protein. * $P < 0.05$, ** $P < 0.01$, *** $P < 0.001$, **** $P < 0.0001$ using two-way ANOVA with Tukey's correction for multiple comparisons. Data are means \pm s.d. BAL samples from all 21 animals ($n = 7$, three groups) were included in the flow cytometry experiments and analyses (a-d). For antigen-specific studies, samples from four animals per group were employed (e-d).

transducing apoptotic signals through activation of caspase 8 (ref. 51) activating CD8 cells⁵² and potentiating IFN- γ -induced killing of *Mtb*^{53,54}. On the other hand, BCG induces strong expression of the SigH regulon (including antioxidants) and is therefore unable to alter these interactions. In fact most BCG strains exhibit duplication of *sigH*, likely rendering it even less susceptible to phagocyte oxidative mechanisms⁵⁵. *In vitro* results thus hint at the mechanism by which pulmonary vaccination with *Mtb* Δ *sigH* could generate protective responses. Unable to counter the host oxidative burst, the mutant elicited greater IL-1 β and TNF- α expression leading to significantly greater antimicrobial response, apoptosis and antigen presentation. That *Mtb* uses Type I signalling to modulate IL-1 β expression is well established⁵⁶.

CD4⁺ T cells play a key role in the control of *Mtb* infection, and polyfunctional cytokine production of antigen-specific Th1 cells is associated with this control⁵⁷. Animals vaccinated with *Mtb* Δ *sigH* displayed higher frequencies of *Mtb* cell wall- and culture filtrate protein-responsive polyfunctional CD4⁺ T cells compared with unvaccinated animals. Recent data have shown that markers of T-cell immune activation in human TB are associated with smear and culture conversion during anti-TB treatment⁵⁸. Nonetheless, the current study had some limitations; for example, protection was only demonstrated in a homologous strain. Thus, future experiments should test the efficacy of the current and related mutants against high-virulence heterologous strains of the same clade as CDC1551, as well as of a different

lineage. Second, a lethal challenge at 8 weeks post vaccination may not sufficiently model protection arising from long-term antigen-specific memory T-cell responses. A prior report suggested that BCG failed to induce long-term central memory responses to *Mtb* infection, which may account for its failure to protect adults against TB¹⁰. Successful vaccination against TB will require elicitation of both a stable and broad repertoire of memory responses to ensure effective protection against the pathogen during a subsequent infection⁴¹. While the current results did not establish long-term immunity based on effective elicitation of T_{CM} responses, the findings did demonstrate that prior pulmonary vaccination with *Mtb* Δ *sigH* resulted in a markedly superior elicitation of both CD4⁺ and CD8⁺ T_{CM} responses relative to BCG vaccination. An abundance of data has indicated that T_{CM} lymphocytes retain a potent proliferative capacity and can differentiate into the T_{EM} phenotype when re-exposed to the cognate antigen⁵⁹. The current data demonstrated that *Mtb* Δ *sigH* elicited a more efficient post-vaccination T_{CM} response, a greater T_{EM} response following challenge and conferred stronger protection. In this study, vaccines were delivered via aerosol, although BCG is given to recipients intradermally. It is impossible to directly compare the results from the aerosol-BCG group to the effectiveness of intradermal BCG vaccination. There have been recent attempts, however, to deliver vaccines, directly to the lung¹¹, driven by the pioneering work of Barclay *et al.*¹², who showed that macaques could be protected against TB by aerosolized BCG. While a direct

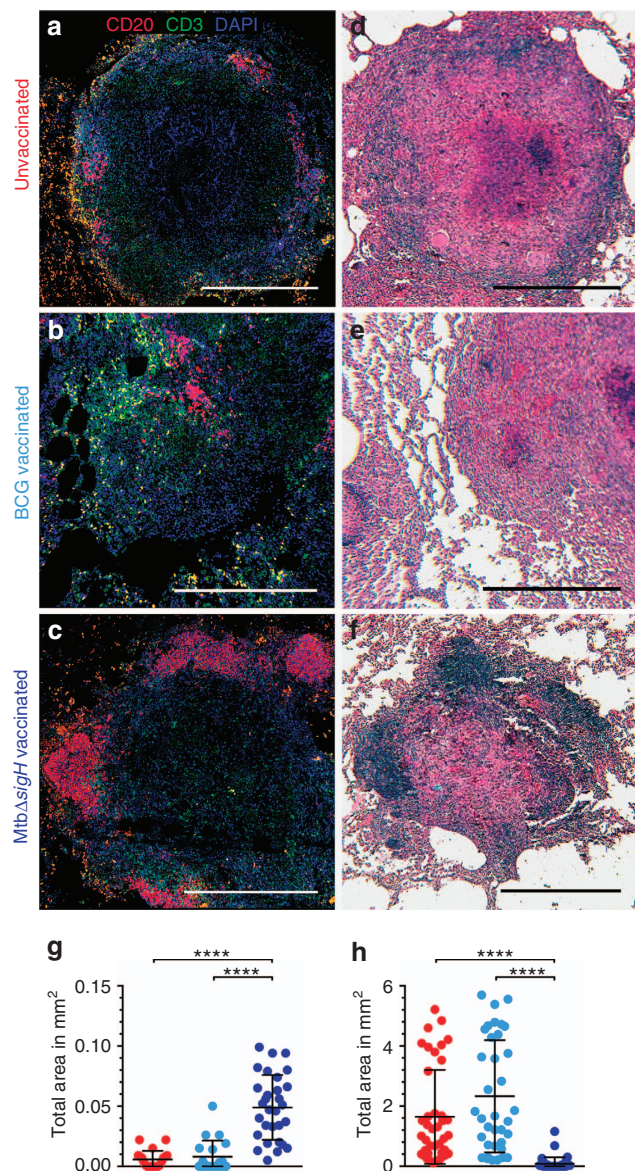


Figure 10 | Induction of BALT after lethal *Mtb* challenge correlates with protection from pulmonary granulomatous TB. (a–c) Co-staining of lung sections with CD3 (green) and CD20 (red) and staining of corresponding sections (d–f) with H&E revealed that (a,d) vaccine-naïve animals and (b,e) BCG-vaccinated animals had significantly reduced iBALT follicle formation in comparison with (c,f) *MtbΔsigH*-vaccinated animals, at necropsy, after lethal *Mtb* challenge. White and black scale bars, 500 μm. Quantification of multiple lesions in six different animals were used the analysis. (g) Total area (mm²) of iBALT follicles and (h) granulomatous pathology in unvaccinated (red), BCG-vaccinated (light blue) and *MtbΔsigH*-vaccinated (dark blue) animals. *****P* < 0.0001 using Student's *t*-test. Data are means ± s.d. At least 10 sections from each slide derived from a lung block from multiple animals in each group were used for statistical analysis (g–h).

comparison of the effectiveness of aerosol-to-intradermal-administered BCG was beyond the scope of this study, preliminary data and prior reports of intradermal BCG vaccination^{14,24,60} suggest that aerosol–BCG outperformed intradermal vaccination in macaques.

Although BCG induces potent cellular responses in infants and protects them, neither the responses nor the efficacy are generally considered to be long lasting⁶¹, although some reports strongly suggest that this is possible⁹. Furthermore, BCG does not

completely protect against pulmonary TB including reactivation and reinfection⁶¹. New vaccines against TB are therefore urgently needed. It has therefore been hypothesized that rationally attenuated strains of *Mtb* are likely better at serving as vaccine platforms against TB, since these strains are human-adapted, in contrast to bovine-adapted BCG⁶¹. There are other issues that limit the effectiveness of BCG. It is only able to induce cytokines associated with long-lasting control of *Mtb* infection several months post vaccination, meanwhile enabling a window of dissemination⁶². Furthermore, *Mtb*, unlike BCG, retains known immunodominant epitopes for humans. Finally, it has been argued that *Mtb* expresses genes important for the evasion of host immune responses. SigH is one such gene allowing the pathogen to significantly induce the expression of thioredoxins, which attenuate phagocyte oxidative burst^{20,22,47}. Thus, *MtbΔsigH*, a human-adapted strain with a significant immune-evasion impairment, is exceedingly safe even after direct high-dose delivery into primate lungs.

In summary, our results provide a roadmap for identifying correlates of protection from TB in a highly human-like model. While it remains to be seen whether such responses can also be elicited following intradermal vaccination, there is considerable renewal of interest in matching the route of vaccination with that of infection in generating protection against TB¹³.

Methods

Nonhuman primates. All animal procedures were approved by the Institutional Animal Care and Use Committee and were performed in strict accordance with the NIH guidelines. Twenty-one specific-pathogen-free, retrovirus-free, mycobacteria-naïve, adult rhesus macaques, bred and housed at the Tulane National Primate Research Centre (TNPRC), between the ages of 3 and 12 years were assigned to three groups of seven on the basis of power calculations, which suggested that statistical significance could be detected with sufficient power in these group sizes if addressing a reduction in the average lung bacterial burden by 1log. One group of macaques (*n* = 7) remained unvaccinated, a second group (*n* = 7) was vaccinated with a target dose of 1,000 CFU of *M. bovis* BCG (Danish) while the third group (*n* = 7) was vaccinated with an equivalent dose of the *MtbΔsigH* isogenic mutant in the CDC1551 background. Aerosol vaccination was conducted using the same equipment and procedural configuration as the *Mtb* challenge component of the study (see below). The average ages of the animals within each group were 7.42 ± 4.26 years for the unvaccinated group, 7.38 ± 4.50 years for the BCG-vaccinated group and 6.75 ± 4.02 years for the *MtbΔsigH* group, and these were not statistically significant differences (Supplementary Fig. 6).

Aerosol procedures for both vaccination and *Mtb* challenge. Animals were both aerosol-vaccinated and challenged with *Mtb* using the same methodology and equipment configuration. A custom head-only dynamic inhalation system housed within a class III biological safety cabinet was used for this purpose⁶³. The use of this inhalation system for aerosol delivery to non human primate (NHP)⁶³ has been described for numerous studies involving *Mtb*^{20,25,29,32} as well as other agents⁶⁴. Initially, the respective microbial efficiencies of *MtbΔsigH* gene mutant and the parental *Mtb* CDC1551 strains were determined through a series of aerosol-only studies. The microbial efficiencies were used to estimate achievable aerosol doses that could be delivered to each animal using mathematical formula catered to this purpose⁶⁵ for both the aerosol vaccination and subsequent challenge experiments. The animal vaccinations (and challenge exposures) were performed singly, and a 'target' dose is reported for the group based on prevailing experimental conditions, including individual animal respiratory rate, during each exposure event. Actual individual dose is based on *post hoc* analysis of active aerosol sampling of the inhalation chamber during the time of each vaccination and bacterial challenge. All aerosol infections were performed in a single day.

Clinical procedures including sampling and euthanasia. Vaccines were delivered directly to the deep lung via the aerosol route in a manner similar to how the *Mtb* challenge is administered. Eight weeks post vaccination, each of the three groups was infected via the inhalation route with a target dose of 1,000 CFU of *Mtb* CDC1551. Samples were collected before vaccination, post vaccination and post infection. For the sake of clarity, results from vaccinated and infected NHPs are reported in two phases: post vaccination, which means after aerosol vaccination with either BCG or *MtbΔsigH*, put before challenge with *Mtb* and post infection (or post challenge), that is, after challenge with *Mtb*.

A tuberculin skin test was performed before vaccination (–2 weeks), post vaccination (3 weeks) and post infection (11 weeks) as previously described by

administration of mammalian tuberculin into the right eyelid^{20,24,25,29,32,33}. Thoracic radiographs (CXRs) were acquired 2 weeks before vaccination and at 3, 7, 11 and 14 weeks post vaccination as previously described^{20,24,25,29,32,66}. Briefly, the CXRs were scored by veterinary clinicians in a blinded manner on a subjective scale of 0–4, with a score of 0 denoting normal lung and a score of 4 denoting severe tuberculous pneumonia and pathology. Before vaccination/infection, all 21 animals received a score of 0, as their lungs were perfectly normal at this time. The following subjective scoring system was used: 0 (no pathological involvement); 1 (mild pathological involvement); 2 (moderate pathological involvement); 3 (extensive pathological involvement) and 4 (severe pathological involvement).

Blood was drawn before vaccination (–2 weeks) and then weekly thereafter for the performance of complete blood count and serum chemistry^{20,24,25,29,32}. Blood collected in EDTA tubes (Sarstedt AG & co.) was used for whole-blood flow cytometry using panels described previously⁶⁷. Blood collected in Cell Preparation tubes (Sarstedt AG & co.) was used to isolate PBMC for antigen-specific assays. BAL samples were obtained as previously described, using two washes of 40-ml sterile saline 2 weeks before vaccination and at 3, 7, 11 and 14 weeks^{20,24,25,29,32} and analysed for CFUs.

Necropsy to collect tissues was performed during euthanasia. There were two different reasons for euthanasia. In all 100% (7/7) unvaccinated control animals, as well as ~57% (4/7) of BCG-vaccinated animals, disease progressed to an extent that humane euthanasia was deemed necessary by clinical veterinarians on this team (Fig. 8h and Supplementary Table 1). These humane end points were pre-defined in the animal-use protocol and applied as a measure of reduction of discomfort. The TNPRC Institutional Animal Care and Use Committee approved all animal-related procedures and activities. BCG-vaccinated (43% (3/7)) and *MtbΔsigH*-vaccinated (100%) animals were either disease-free or had not progressed to an extent that required humane euthanasia till day 60. Such animals were euthanized for tissue collection via necropsy at that point (between days 60 and 62). At necropsy, lung, spleen and liver tissues were collected and processed as previously described, and CFUs were determined per gram of tissue, using four pooled lung samples per animal, each of which comprised five sections each, thus representing every lung lobe with at least one sample^{20,24,25,29,32}. A subset of colonies obtained post-challenge necropsy was assayed for resistance to hygromycin to classify them as residual *MtbΔsigH*, and subjected to PCR for *sigH* and *esat6* to classify them as residual *MtbΔsigH* and BCG, respectively. No evidence of residual *MtbΔsigH* or BCG was found. End point criteria for euthanasia were previously described. Briefly, animals were euthanized if they exhibited four or more of the following: (I) a 2 °F increase in body temperature relative to pre-infection values that persisted for three or more consecutive weeks; (II) a 15% or greater loss in body weight; (III) serum CRP values greater than 10 mg ml⁻¹ for two or more consecutive readings; (IV) CXR values higher than 2; (V) respiratory discomfort resulting in vocalization; (VI) significant-to-complete loss of appetite; and (VII) detectable bacilli in BAL samples. CRP values were included as criteria for euthanasia because CRP is a marker for systemic inflammation that exhibits a high degree of correlation with active TB in macaques^{20,24,25,29,32,33}. Lung pathology at necropsy was determined as described earlier^{21,26,29,30,38} using stereological principles described by Sharpe *et al.*²⁷. Briefly, lung involvement was quantified by point counting using an overlaid grid with 18.5-mm point spacing. Towards this end, digital images of three systematic random microscopic fields with an original magnification of ×2.5 per slide were employed. At least one sample from each of the four lobes of each lung was used. Intersections representing normal lung included interstitium and air space, while lesions comprised intersections with massive areas of inflammatory cells, haemorrhage, oedema, necrosis or individual to multifocal to lobar granulomas. Differences between completely normal and somewhat inflamed airspace containing localized, small zones of subacute inflammation sans fibrous or cellular encapsulation were not differentiated.

Transcriptomics. BAL samples were obtained from animals before vaccination (–2 weeks), post vaccination (weeks 3 and 7) and post infection (weeks 11 and 14) as previously described^{20,24,25,29,32,33,68}. For stabilization, 8 ml of 100% fetal bovine serum (Invitrogen, Life Sciences) was immediately added to 80 ml of the BAL sample. The sample was centrifuged at 400 r.p.m. for 10 min at 4 °C in an Allegra benchtop centrifuge. The pelleted cells were washed with cold RPMI media (Invitrogen, Life Sciences) and stored at –80 °C until analysis. For transcriptomics, total macaque RNA was isolated from total BAL obtained at the pre-vaccination and the 3 week post-vaccination time points as previously described³⁰ using an RNeasy kit (Qiagen), followed by RNA amplification (Ambion MessageAmp). The cDNA derived from the amplified RNA samples from pre-vaccination time points were labelled with Cy3, and samples from the 3-week post-vaccination time point were labelled with Cy5 (Agilent Technologies). Microarray analyses were performed as previously described by assessing the relative expression of transcripts in the Cy5 (experimental)-labelled samples relative to the Cy3(control)-labelled samples, using Agilent 4 × 44k Rhesus Monkey microarrays^{20,24,25,68}. Global impact of expression profiles was analysed using Database for Annotation, Visualization and Integrated Discovery (DAVID)³⁰.

iBALT. Immunofluorescence confocal microscopy was used to measure iBALT as previously described using formalin-fixed, paraffin-embedded tissue^{31,69}.

Flow cytometry. Flow cytometry was performed on whole-blood and BAL samples obtained from all 21 animals as previously described^{25,33}. For T-cell phenotyping, the following antibodies were used: CD3 V500 (1:50, clone SP34-2), CD4 PerCP-Cy5.5 (1:10, clone L200), CD8 PE-TxRed (1:30, clone RPA-T8), CD28 APC (1:5, clone CD28.2), CD69 APC-Cy7 (1:20, clone FN50), CD95 PE-Cy5 (1:5, clone DX2), CD183 AL488 (1:10, clone 1C6/CXCR3), CD184 PE-Cy5 (1:5, clone 12G5), CD195 APC (1:5, clone 3A9), CD197 PE-Cy7 (1:20, clone 3D12), HLA-DR APC-Cy7 (1:75, clone L243) and Ki67 PE-Cy7 (1:50, clone B56) all purchased from BD Biosciences (San Jose, CA, USA). Flow cytometry analyses were conducted by gating first on lymphocytes followed by the elimination of B cells by gating for CD20. The remaining cells were gated for the selection of T cells using CD3, followed by gating into CD3⁺CD4⁺ and CD3⁺CD8⁺ subpopulations. The frequencies of CD4⁺ and CD8⁺ T cells expressing activation and homing markers were compared using Ki67, CXCR3, CCR5 and CCR7 (ref. 70). The levels of Foxp3⁺ were determined as a measure of the T_{Reg} response. Finally, the extent of CD4⁺ and CD8⁺ cells belonging to either T_{CM} or T_{EM} relative to the naive T-cell population were measured using a combination of CD28 and CD95 markers³⁷.

Antigen-specific immune response. PBMCs isolated from whole blood collected from unvaccinated, vaccinated and infected NHPs were stimulated with *Mtb* cell wall extract (BEI Resources) for the performance of intracellular cytokine staining as previously described, using *Mtb* cell filtrate protein and cell wall extract for stimulation⁵⁷.

In vitro infection of rhesus macaque BMDMs. Rh-BMDMs were generated and infected with *Mtb* CDC1551, the isogenic *MtbΔsigH* mutant in this strain, and BCG at a multiplicity of infection of 1:10 as previously described, for 4 h (refs 22,46). CFUs were measured as described at different time points including 4, 24, 48, 72, 96 and 120 h. CXCL13 expression was measured using DNA microarray²⁵ and quantitative RT-PCR²². The expression of pro-inflammatory mediators TNF-α, IL-1β and IL-6 was measured using real-time RT-PCR as described earlier²². The expression of specific chemokines, for example, CXCL9 and CXCL10, was measured using the Cytokine Monkey Magnetic 29-Plex Panel kit from Life-Tech, essentially as described earlier²².

Statistical analyses. Statistical comparisons were performed using one-way or two-way ANOVA in GraphPad Prism with Sidak's correction for multiple hypotheses. Analysis of transcriptome data was performed using Spotfire DecisionSite^{24,25,68} LOWESS scripts, Ingenuity Pathways Analysis and DAVID as previously described²⁵. Specifically, genes with twofold or greater induction in triplicate samples from either vaccination were uploaded to DAVID, and statistically significant accumulation of terms calculated.

References

- Zumla, A. *et al.* The WHO 2014 global tuberculosis report-further to go. *Lancet Glob Health* **3**, e10–12 (2015).
- Kaufmann, S. H. *et al.* Progress in tuberculosis vaccine development and host-directed therapies—a state of the art review. *Lancet Respir. Med.* **2**, 301–320 (2014).
- Orme, I. M. Prospects for new vaccines against tuberculosis. *Trends Microbiol.* **3**, 401–404 (1995).
- Hingley-Wilson, S. M., Sambandamurthy, V. K. & Jacobs, Jr. W. R. Survival perspectives from the world's most successful pathogen, *Mycobacterium tuberculosis*. *Nat. Immunol.* **4**, 949–955 (2003).
- Kaufmann, S. H. *et al.* Progress in tuberculosis vaccine development and host-directed therapies—a state of the art review. *Lancet Respir. Med.* **2**, 301–320 (2014).
- Wilkie, M. E. & McShane, H. TB vaccine development: where are we and why is it so difficult? *Thorax* **70**, 299–301 (2015).
- Tameris, M. D. *et al.* Safety and efficacy of MVA85A, a new tuberculosis vaccine, in infants previously vaccinated with BCG: a randomised, placebo-controlled phase 2b trial. *Lancet* **381**, 1021–1028 (2013).
- McShane, H. *et al.* BCG: myths, realities, and the need for alternative vaccine strategies. *Tuberculosis (Edinb)* **92**, 283–288 (2012).
- Aronson, N. E. *et al.* Long-term efficacy of BCG vaccine in American Indians and Alaska Natives: A 60-year follow-up study. *JAMA* **291**, 2086–2091 (2004).
- Henaio-Tamayo, M., Ordway, D. J. & Orme, I. M. Memory T cell subsets in tuberculosis: what should we be targeting? *Tuberculosis (Edinb)* **94**, 455–461 (2014).
- García-Contreras, L. *et al.* Immunization by a bacterial aerosol. *Proc. Natl Acad. Sci. USA* **105**, 4656–4660 (2008).
- Barclay, W. R. *et al.* Protection of monkeys against airborne tuberculosis by aerosol vaccination with bacillus Calmette-Guerin. *Am. Rev. Respir. Dis.* **107**, 351–358 (1973).
- Manjaly Thomas, Z. R. & McShane, H. Aerosol immunisation for TB: matching route of vaccination to route of infection. *Trans. R Soc. Trop. Med. Hyg.* **109**, 175–181 (2015).

14. Darrah, P. A. *et al.* Aerosol vaccination with AERAS-402 elicits robust cellular immune responses in the lungs of rhesus macaques but fails to protect against high-dose *Mycobacterium tuberculosis* challenge. *J. Immunol.* **193**, 1799–1811 (2014).
15. Larsen, M. H. *et al.* Efficacy and safety of live attenuated persistent and rapidly cleared *Mycobacterium tuberculosis* vaccine candidates in non-human primates. *Vaccine* **27**, 4709–4717 (2009).
16. Russell, D. G. The evolutionary pressures that have molded *Mycobacterium tuberculosis* into an infectious adjuvant. *Curr. Opin. Microbiol.* **16**, 78–84 (2013).
17. Hmama, Z., Pena-Diaz, S., Joseph, S. & Av-Gay, Y. Immuno-evasion and immunosuppression of the macrophage by *Mycobacterium tuberculosis*. *Immunol. Rev.* **264**, 220–232 (2015).
18. Kaushal, D. *et al.* Reduced immunopathology and mortality despite tissue persistence in a *Mycobacterium tuberculosis* mutant lacking alternative sigma factor, SigH. *Proc. Natl Acad. Sci. USA* **99**, 8330–8335 (2002).
19. Hernandez Pando, R., Aguilar, L. D., Smith, I. & Manganelli, R. Immunogenicity and protection induced by a *Mycobacterium tuberculosis* sigE mutant in a BALB/c mouse model of progressive pulmonary tuberculosis. *Infect. Immun.* **78**, 3168–3176 (2010).
20. Mehra, S. *et al.* The *Mycobacterium tuberculosis* stress response factor SigH is required for bacterial burden as well as immunopathology in primate lungs. *J. Infect. Dis.* **205**, 1203–1213 (2012).
21. Manganelli, R. *et al.* Role of the extracytoplasmic-function sigma factor sigma(H) in *Mycobacterium tuberculosis* global gene expression. *Mol. Microbiol.* **45**, 365–374 (2002).
22. Dutta, N. K. *et al.* The stress-response factor SigH modulates the interaction between *Mycobacterium tuberculosis* and host phagocytes. *PLoS ONE* **7**, e28958 (2012).
23. Barclay, W. R., Anacker, R. L., Brehmer, W., Leif, W. & Ribic, E. Aerosol-induced tuberculosis in subhuman primates and the course of the disease after intravenous BCG vaccination. *Infect. Immun.* **2**, 574–582 (1970).
24. Mehra, S. *et al.* Granuloma correlates of protection against tuberculosis and mechanisms of immune modulation by *Mycobacterium tuberculosis*. *J. Infect. Dis.* **207**, 1115–1127 (2013).
25. Mehra, S. *et al.* The DosR regulon modulates adaptive immunity and is essential for *M. tuberculosis* persistence. *Am. J. Respir. Crit. Care Med.* **191**, 1185–1196 (2015).
26. Kaushal, D., Mehra, S., Didier, P. J. & Lackner, A. A. The non-human primate model of tuberculosis. *J. Med. Primatol.* **41**, 191–201 (2012).
27. Sharpe, S. A. *et al.* Determination of lesion volume by MRI and stereology in a macaque model of tuberculosis. *Tuberculosis (Edinb)* **89**, 405–416 (2009).
28. Diedrich, C. R. *et al.* Reactivation of latent tuberculosis in cynomolgus macaques infected with SIV is associated with early peripheral T cell depletion and not virus load. *PLoS ONE* **5**, e9611 (2010).
29. Mehra, S. *et al.* Reactivation of latent tuberculosis in rhesus macaques by coinfection with simian immunodeficiency virus. *J. Med. Primatol.* **40**, 233–243 (2011).
30. Kamath, A. T. *et al.* New live mycobacterial vaccines: the Geneva consensus on essential steps towards clinical development. *Vaccine* **23**, 3753–3761 (2005).
31. Slight, S. R. *et al.* CXCR5(+) T helper cells mediate protective immunity against tuberculosis. *J. Clin. Invest.* **123**, 712–726 (2013).
32. Dutta, N. K. *et al.* Genetic requirements for the survival of tubercle bacilli in primates. *J. Infect. Dis.* **201**, 1743–1752 (2010).
33. Phillips, B. L. *et al.* LAG3 expression in active *Mycobacterium tuberculosis* infections. *Am. J. Pathol.* **185**, 820–833 (2015).
34. Jayaraman, P. *et al.* IL-1beta promotes antimicrobial immunity in macrophages by regulating TNFR signaling and caspase-3 activation. *J. Immunol.* **190**, 4196–4204 (2013).
35. Manca, C. *et al.* Hypervirulent *M. tuberculosis* W/Beijing strains upregulate type I IFNs and increase expression of negative regulators of the Jak-Stat pathway. *J. Interferon Cytokine Res.* **25**, 694–701 (2005).
36. Mayer-Barber, K. D. *et al.* Host-directed therapy of tuberculosis based on interleukin-1 and type I interferon cross-talk. *Nature* **511**, 99–103 (2014).
37. Pitcher, C. J. *et al.* Development and homeostasis of T cell memory in rhesus macaque. *J. Immunol.* **168**, 29–43 (2002).
38. Moyron-Quiroz, J. E. *et al.* Role of inducible bronchus associated lymphoid tissue (iBALT) in respiratory immunity. *Nat. Med.* **10**, 927–934 (2004).
39. Fairfax, K. C. *et al.* IL-4-secreting secondary T follicular helper (Tfh) cells arise from memory T cells, not persisting Th cells, through a B cell-dependent mechanism. *J. Immunol.* **194**, 2999–3010 (2015).
40. Phuath, J. Y., Mattila, J. T., Lin, P. L. & Flynn, J. L. Activated B cells in the granulomas of nonhuman primates infected with *Mycobacterium tuberculosis*. *Am. J. Pathol.* **181**, 508–514 (2012).
41. Nunes-Alves, C. *et al.* In search of a new paradigm for protective immunity to TB. *Nat. Rev. Microbiol.* **12**, 289–299 (2014).
42. Kohlmeier, J. E. *et al.* Inflammatory chemokine receptors regulate CD8(+) T cell contraction and memory generation following infection. *J. Exp. Med.* **208**, 1621–1634 (2011).
43. Caruso, A. M. *et al.* Mice deficient in CD4 T cells have only transiently diminished levels of IFN-gamma, yet succumb to tuberculosis. *J. Immunol.* **162**, 5407–5416 (1999).
44. Chen, C. Y. *et al.* A critical role for CD8 T cells in a nonhuman primate model of tuberculosis. *PLoS Pathog.* **5**, e1000392 (2009).
45. Mehra, S. & Kaushal, D. Functional genomics reveals extended roles of the *Mycobacterium tuberculosis* stress response factor sigmaH. *J. Bacteriol.* **191**, 3965–3980 (2009).
46. Mehra, S., Dutta, N. K., Mollenkopf, H. J. & Kaushal, D. *Mycobacterium tuberculosis* MT2816 encodes a key stress-response regulator. *J. Infect. Dis.* **202**, 943–953 (2010).
47. Kernodle, D. S. SigH, antioxidants, and the pathogenesis of pulmonary tuberculosis. *J. Infect. Dis.* **205**, 1186–1188 (2012).
48. Winaw, F., Hegasy, G., Kaufmann, S. H. & Schaible, U. E. No life without death—apoptosis as prerequisite for T cell activation. *Apoptosis* **10**, 707–715 (2005).
49. Obst, R. *et al.* Sustained antigen presentation can promote an immunogenic T cell response, like dendritic cell activation. *Proc. Natl Acad. Sci. USA* **104**, 15460–15465 (2007).
50. Harris, J. & Keane, J. How tumour necrosis factor blockers interfere with tuberculosis immunity. *Clin. Exp. Immunol.* **161**, 1–9 (2010).
51. Wajant, H., Pfizenmaier, K. & Scheurich, P. Tumor necrosis factor signaling. *Cell. Death Differ.* **10**, 45–65 (2003).
52. Bruns, H. *et al.* Anti-TNF immunotherapy reduces CD8+ T cell-mediated antimicrobial activity against *Mycobacterium tuberculosis* in humans. *J. Clin. Invest.* **119**, 1167–1177 (2009).
53. Harris, J., Hope, J. C. & Keane, J. Tumor necrosis factor blockers influence macrophage responses to *Mycobacterium tuberculosis*. *J. Infect. Dis.* **198**, 1842–1850 (2008).
54. Schaible, U. E., Sturgill-Koszycki, S., Schlesinger, P. H. & Russell, D. G. Cytokine activation leads to acidification and increases maturation of *Mycobacterium avium*-containing phagosomes in murine macrophages. *J. Immunol.* **160**, 1290–1296 (1998).
55. Kernodle, D. S. Decrease in the effectiveness of Bacille Calmette-Guérin vaccine against pulmonary tuberculosis: a consequence of increased immune suppression by microbial antioxidants, not overattenuation. *Clin. Infect. Dis.* **51**, 177–184 (2010).
56. Novikov, A. *et al.* *Mycobacterium tuberculosis* triggers host type I IFN signaling to regulate IL-1beta production in human macrophages. *J. Immunol.* **187**, 2540–2547 (2011).
57. Adekambi, T. *et al.* Distinct effector memory CD4+ T cell signatures in latent *Mycobacterium tuberculosis* infection, BCG vaccination and clinically resolved tuberculosis. *PLoS ONE* **7**, e36046 (2012).
58. Riou, C. *et al.* A subset of circulating blood mycobacteria-specific CD4 T cells can predict the time to *Mycobacterium tuberculosis* sputum culture conversion. *PLoS ONE* **9**, e102178 (2014).
59. Hamilton, S. E. & Jameson, S. C. CD8 T cell memory: it takes all kinds. *Front. Immunol.* **3**, 353 (2012).
60. Lin, P. L. *et al.* The multistage vaccine H56 boosts the effects of BCG to protect cynomolgus macaques against active tuberculosis and reactivation of latent *Mycobacterium tuberculosis* infection. *J. Clin. Invest.* **122**, 303–314 (2012).
61. Ottenhoff, T. H. & Kaufmann, S. H. Vaccines against tuberculosis: where are we and where do we need to go? *PLoS Pathog.* **8**, e1002607 (2012).
62. Cruz, A. *et al.* BCG vaccination-induced long-lasting control of *Mycobacterium tuberculosis* correlates with the accumulation of a novel population of CD4(+)IL-17(+)TNF(+)IL-2(+) T cells. *Vaccine* **33**, 85–91 (2015).
63. Hartings, J. M. & Roy, C. J. The automated bioaerosol exposure system: preclinical platform development and a respiratory dosimetry application with nonhuman primates. *J. Pharmacol. Toxicol. Methods* **49**, 39–55 (2004).
64. Roy, C. J. *et al.* Thermostable ricin vaccine protects rhesus macaques against aerosolized ricin: epitope-specific neutralizing antibodies correlate with protection. *Proc. Natl Acad. Sci. USA* **112**, 3782–3787 (2015).
65. Swearingen, J. R. *Biodefense: Research Methodology and Animal Models* 2nd edn (Taylor & Francis, 2012).
66. Darrah, P. A. *et al.* Aerosol vaccination with AERAS-402 elicits robust cellular immune responses in the lungs of rhesus macaques but fails to protect against high-dose *Mycobacterium tuberculosis* challenge. *J. Immunol.* **193**, 1799–1811 (2014).
67. Dutta, N. K., McLachlan, J., Mehra, S. & Kaushal, D. Humoral and lung immune responses to *Mycobacterium tuberculosis* infection in a primate model of protection. *Trials Vaccinol.* **3**, 47–51 (2014).
68. Mehra, S. *et al.* Transcriptional reprogramming in nonhuman primate (rhesus macaque) tuberculosis granulomas. *PLoS ONE* **5**, e12266 (2010).
69. Gopal, R. *et al.* S100A8/A9 proteins mediate neutrophilic inflammation and lung pathology during tuberculosis. *Am. J. Respir. Crit. Care Med.* **188**, 1137–1146 (2013).
70. Veazey, R. S. *et al.* Dynamics of CCR5 expression by CD4(+) T cells in lymphoid tissues during simian immunodeficiency virus infection. *J. Virol.* **74**, 11001–11007 (2000).

Acknowledgements

This research was supported by startup funds and a Center for Biomedical Research Excellence (COBRE) award to S.M. (P30GM110760), awards to D.K. (AI089323, HL106790, HL106790-S1, AI111943 and RR026006), S.A.K. and D.K. (AI111914) and the TNPRC (OD011104 and AI058609), including its pilot programme, the Emory Center for AIDS Research (CFAR; AI050409), the Louisiana Board of Regents and the Tulane Office of the Vice-President for Research.

Author contributions

D.K. provided funding, advised on the experimental design, carried out the experiments, analysed the results and participated in the manuscript preparation; T.W.F. carried out the experiments, analysed the results and participated in the manuscript preparation; U.S.G. carried out the experiments and analysed results; X.A. carried out the experiments and analysed results; T.A. carried out the experiments and analysed results; J.R.-M. carried out the experiments; N.A.G. carried out the experiments; A.-M.F.J. carried out the experiments; B.L.P. carried out the experiments; M.H.A. carried out the experiments; K.E.R.-L. provided veterinary assistance; L.A.D. provided veterinary assistance; C.J.R. carried out experiments; P.J.D. performed veterinary pathology; J.L.B. provided veterinary assistance; J.R. analysed the results; A.A.L. performed veterinary pathology and assisted in data interpretation and the manuscript preparation; S.A.K. provided funding and assisted in data interpretation and manuscript preparation; S.M. provided funding, advised on the experimental design, analysed the results and participated in the manuscript preparation. All authors reviewed the manuscript before submission.

Additional information

Accession codes: DNA microarray data have been deposited in the Gene Expression Omnibus under the Accession number GPL10183.

Supplementary Information accompanies this paper at <http://www.nature.com/naturecommunications>

Competing financial interests: The authors declare no competing financial interests.

Reprints and permission information is available online at <http://npg.nature.com/reprintsandpermissions/>

How to cite this article: Kaushal, D. *et al.* Mucosal vaccination with attenuated *Mycobacterium tuberculosis* induces strong central memory responses and protects against tuberculosis. *Nat. Commun.* 6:8533 doi: 10.1038/ncomms9533 (2015).



This work is licensed under a Creative Commons Attribution 4.0 International License. The images or other third party material in this article are included in the article's Creative Commons license, unless indicated otherwise in the credit line; if the material is not included under the Creative Commons license, users will need to obtain permission from the license holder to reproduce the material. To view a copy of this license, visit <http://creativecommons.org/licenses/by/4.0/>